EUROPEAN TRANSACTIONS ON TELECOMMUNICATIONS
Eur. Trans. Telecomms. 2008; **19**:751–759
Published online 29 September 2008 in Wiley InterScience
(www.interscience.wiley.com) DOI: 10.1002/ett.1321

Blind channel identification in Alamouti coded systems: a comparative study of eigendecomposition methods in indoor transmissions at 2.4 GHz†

Héctor J. Pérez-Iglesias[1], José A. García-Naya[1], Adriana Dapena[1]*, Luis Castedo[1] and Vicente Zarzoso[2]

[1]*Departamento de Electrónica y Sistemas, Universidade da Coruña, Facultad de Informática, Campus de Elviña, no. 5, 15071 A Coruña, Spain*
[2]*Laboratoire I3S, Université de Nice-Sophia Antipolis, Les Algorithmes, Euclide-B, BP 121 06903 Sophia Antipolis, France*

SUMMARY

This paper focuses on blind channel estimation in Alamouti coded systems with one receiving antenna working in indoor scenarios where the flat fading assumption is reasonable. A comparative study of several channel estimation techniques in both simulated and realistic scenarios is presented. The tested methods exploit the orthogonality property of the Alamouti coded channel matrix, and are based on the eigendecomposition of a square matrix made up of second-order statistics (SOS) or higher order statistics (HOS) of the observed signals. An experimental evaluation is carried out on a testbed developed at the University of A Coruña (UDC) and operating at 2.4 GHz. The results show the superior performance of the SOS-based blind channel estimation technique in both line of sight (LOS) and non-LOS (NLOS) channels.

1. INTRODUCTION

During the last decade, a large number of space-time coding (STC) techniques have been proposed to exploit the spatial diversity in multiple input multiple output (MIMO) wireless communication systems that employ multiple antennas at both transmission and reception (see, for instance, References [1, 2] and references therein). A remarkable example is orthogonal space time block coding (OSTBC) because it is able to provide full transmit diversity without any channel state information (CSI) at transmission and with very simple encoding and decoding procedures [3, 4]. The basic premise of OSTBC is the encoding of the transmitted symbols into an orthogonal matrix which reduces the optimum maximum likelihood (ML) decoder to a matrix-matched filter followed by a symbol-by-symbol detector.

The OSTBC scheme for MIMO systems with two transmit antennas is known as the Alamouti code [3] and it is the only OSTBC capable of achieving full spatial rate for complex constellations. Other OSTBCs have been proposed for more than two transmit antennas but they suffer from severe spatial rate loss [4, 5]. The Alamouti code can be used in systems with one or multiple antennas at the receiver. Here, (2×1) Alamouti coded systems are used due to their simplicity and their ability to provide maximum diversity gain while achieving the full available channel capacity. It should be noted that Alamouti schemes do not achieve the full potential capacity with more than one receive antenna [6], although the difference is small and of course both diversity and capacity are significantly increased with more than one receive antenna. Because of these advantages, the Alamouti code has been incorporated in the IEEE 802.11 and IEEE 802.16 standards [7].

Coherent detection in (2×1) Alamouti coded systems requires the identification of a (2×2) unitary channel matrix. The standard way to estimate this channel matrix is through the transmission of pilot symbols, also referred to as training sequences. However, the inclusion of pilot symbols reduces the system throughput (equivalently, it reduces the

* Correspondence to: Adriana Dapena, Departamento de Electrónica y Sistemas, Universidade da Coruña, Facultad de Informática, Campus de Elviña, no. 5, 15071 A Coruña, Spain. E-mail: adriana@udc.es
† A previous version of this paper was presented in the 13th European Wireless Conference (EW 2007), Paris, France.

 Accepted 16 June 2008

system spectral efficiency) and wastes transmission energy because training sequences do not convey information. One way to avoid this limitation is the utilisation of differential STBC (DSTBC) [8], a generalisation of differential modulations to the transmission over MIMO channels. Indeed, DSTBCs can be incoherently decoded without the aid of channel estimates but at the cost of a 3-dB performance penalty when compared to coherent detection.

Alternatively, training sequences can be avoided by the use of blind channel identification methods. Although a lot of techniques exist in the literature, in this paper we focus on blind channel estimation methods that are based on the eigenvector decomposition of a (2×2) matrix because of their good trade-off between complexity and performance. In particular, we propose novel methods based on diagonalising matrices containing second-order statistics (SOS) and higher order statistics (HOS) of the receiving signals. These methods, originally proposed in Reference [9], are particularly suitable for the application at hand for three reasons: they exploit the orthogonal property of the channel matrix to be identified; their complexity is very low and they provide an adequate channel estimation for small data blocks. We also consider the method proposed by Beres and Adve [10] for OSTBC which has similar complexity load. As a benchmark, we compare the results with the joint approximate diagonalisation of eigenmatrices (JADE) algorithm [11] although its feasibility in real-time systems is very limited due to its high complexity.

In this paper, we evaluate the performance of the blind channel estimation techniques over both computer simulated flat fading channels and realistic indoor scenarios. For this latter performance evaluation, we have used a MIMO hardware demonstrator developed at the University of A Coruña (UDC), Spain, that operates at the 2.4 GHz Industrial, Scientific and Medical (ISM) band. The evaluation results show the superior performance of the SOS-based method and its ability to approach the same performance as if the channel were least squares (LS) estimated with long training sequences. The SOS-based method is also the least computationally demanding of all compared techniques.

This paper is structured as follows. Section 2 presents the signal model of a (2×1) Alamouti coded system. Section 3 explains the blind methods used to estimate the channel matrix. Section 4 presents the performance results obtained by means of computer simulations. Section 5 describes the MIMO testbed and presents the obtained experimental results. Finally, Section 6 is devoted to the conclusions.

Notations. Throughout this work, boldface uppercase letters are used to denote matrices, for example $\mathbf{X}$, with elements $x_{i,j}$; boldface lowercase letters for column vectors, for example $\mathbf{x}$, and lightface lowercase letters for scalar quantities. Superscripts $(\cdot)^*$, $(\cdot)^{\mathrm{T}}$ and $(\cdot)^{\mathrm{H}}$ represent the conjugate, transpose and Hermitian operators, respectively. The identity matrix of dimensions $(p \times p)$ will be denoted as $\mathbf{I}_p$ and $\mathrm{E}[\cdot]$ stands for the expectation operator.

2. ALAMOUTI CODED SYSTEMS

Figure 1 depicts the baseband representation of an Alamouti coded system with one receiving antenna. Each pair of symbols $\{s_1, s_2\}$ is transmitted in two adjacent periods using a simple strategy: in the first period s_1 and s_2 are transmitted

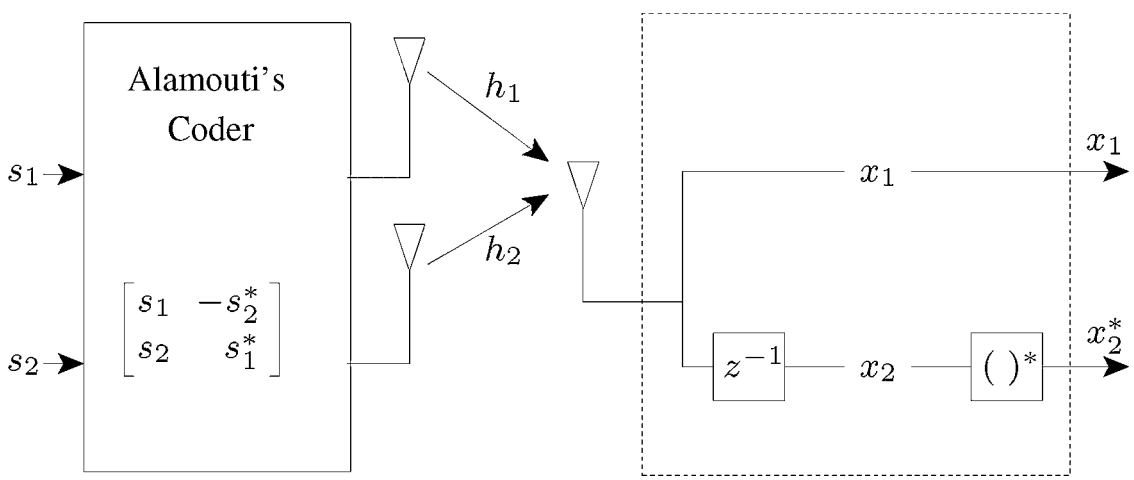

Figure 1. Block diagram of the 2×1 Alamouti coded system.

DOI: 10.1002/ett

through the first and second antennas, respectively, and in the second period $-s_2^*$ is transmitted through the first antenna and s_1^* from the second one. We assume that the exact probability density function of s_i is unknown although they take values from the alphabet of a typical complex modulation such as QAM or PSK. The data sequence is assumed to be composed of independent and identically distributed symbols, so that s_1 and s_2 are statistically independent.

In indoor scenarios, the delay spread of the different multipaths is rather small so it is natural to model the wireless channel as flat fading: the transmitted symbols arrive at the receiving antenna through the fading paths h_1 and h_2. Thus, the signal received during the first period is $x_1 = s_1 h_1 + s_2 h_2 + n_1$. Assuming that the channel remains unchanged, the observation in the second period is given by $x_2 = s_1^* h_2 - s_2^* h_1 + n_2$. Defining the observation vector as $\mathbf{x} = [x_1 \;\; x_2^*]^{\mathrm{T}}$, we obtain that the relationship between the observation vector $\mathbf{x}$ and the source vector $\mathbf{s} = [s_1 \;\; s_2]^{\mathrm{T}}$ is given by

$$\mathbf{x} = \mathbf{H}\mathbf{s} + \mathbf{n} \tag{1}$$

where $\mathbf{H}$ is the (2×2) effective channel matrix,

$$\mathbf{H} = \begin{bmatrix} h_1 & h_2 \\ h_2^* & -h_1^* \end{bmatrix} \tag{2}$$

and where $\mathbf{n} = [n_1 \;\; n_2^*]^{\mathrm{T}}$ is the AWGN modelled as a vector of two uncorrelated zero-mean, complex-valued, circularly symmetric, Gaussian distributed random processes. It is interesting to note that $\mathbf{H}$ is an orthogonal matrix, that is $\mathbf{H}\mathbf{H}^{\mathrm{H}} = \mathbf{H}^{\mathrm{H}}\mathbf{H} = \|\mathbf{h}\|^2 \mathbf{I}_2$ where $\|\mathbf{h}\|^2 = |h_1|^2 + |h_2|^2$ is the squared Euclidean norm of $\mathbf{h}$.

Filtering $\mathbf{x}$ with the matrix-matched filter yields the following decision statistics

$$\mathbf{y} = \mathbf{H}^{\mathrm{H}}\mathbf{x} = \|\mathbf{h}\|^2 \mathbf{s} + \tilde{\mathbf{n}} \tag{3}$$

where $\tilde{\mathbf{n}} = \mathbf{H}^{\mathrm{H}}\mathbf{n}$ is the output noise vector, with the same statistical properties as the input noise. It is apparent from Equation (3) that ML detection of s_1 and s_2 can be calculated by applying $\mathbf{y}$ to a pair of independent scalar slicers. Consequently, the correct detection of the transmitted symbols $\mathbf{s}$ requires the accurate estimation of the channel matrix $\mathbf{H}$ from the received data $\mathbf{x}$.

3. MIMO CHANNEL ESTIMATION

This section describes the channel estimation techniques that will be tested in Sections 4 and 5. The methods are based on computing a (2×2) squared matrix, $\mathbf{C}$, containing SOS or HOS of the received signals. The basic premise of the considered methods is that $\mathbf{C}$ has an algebraic structure of the form $\mathbf{H}\boldsymbol{\Delta}\mathbf{H}^{\mathrm{H}}$ where $\boldsymbol{\Delta}$ is a diagonal matrix. Due to the orthogonal structure of $\mathbf{H}$, if the diagonal entries of $\boldsymbol{\Delta}$ are different, the channel matrix can be identified from the eigenvectors of $\mathbf{C}$ with a possible change of scale and permutation.

3.1. SOS-based approach

We will start by describing a method that estimates the channel from the eigenvectors of the observations autocorrelation matrix. Unlike other SOS-based algorithms [12, 13], this method does not require the use of an additional outer encoder.

According to the signal model in Equation (1), the observations autocorrelation matrix can be written as

$$\mathbf{C}_{\mathrm{SOS}} = \mathrm{E}[\mathbf{x}\mathbf{x}^{\mathrm{H}}] = \mathbf{H}\mathbf{R}_{\mathbf{s}}\mathbf{H}^{\mathrm{H}} + \sigma_n^2 \mathbf{I}_2 \tag{4}$$

where σ_n^2 is the noise power and $\mathbf{R}_{\mathbf{s}} = \mathrm{E}[\mathbf{s}\mathbf{s}^{\mathrm{H}}]$ is the correlation matrix of the transmitted signals. Since $\mathbf{H}$ is orthogonal, Equation (4) can be rewritten as the following eigenvalue decomposition:

$$\mathbf{C}_{\mathrm{SOS}} = \mathbf{H}\left(\mathbf{R}_{\mathbf{s}} + \frac{\sigma_n^2}{\|\mathbf{h}\|^2}\mathbf{I}_2\right)\mathbf{H}^{\mathrm{H}} \tag{5}$$

Notice that if the two transmitted sources have the same power $\mathbf{C}_{\mathrm{SOS}}$ is diagonal and, as a consequence, $\mathbf{H}$ is not identifiable from an eigenvalue decomposition.

For the system to be identifiable, we propose to unbalance the power of the transmitted sources as follows:

$$\mathrm{E}[|s_1'|^2] = \frac{2\sigma_s^2}{1+\gamma^2}, \quad \mathrm{E}[|s_2'|^2] = \frac{2\gamma^2\sigma_s^2}{1+\gamma^2} \tag{6}$$

where $0 < \gamma^2 < 1$ and s_1', s_2' are the new unbalanced sources. In spite of the power unbalancing, notice that the total mean power remains unchanged (i.e. σ_s^2). Now, the eigenvalue decomposition of $\mathbf{C}_{\mathrm{SOS}}$ is

$$\mathbf{C}_{\mathrm{SOS}} = \sigma_s^2 \mathbf{H}\boldsymbol{\Delta}_{\mathrm{SOS}}\mathbf{H}^{\mathrm{H}} \tag{7}$$

DOI: 10.1002/ett

where

$$\mathbf{\Delta}_{\mathrm{SOS}} = \begin{bmatrix} 1+\sigma_h^2 & 0 \\ 0 & \gamma^2+\sigma_h^2 \end{bmatrix} \tag{8}$$

contains the eigenvalues of $\mathbf{C}_{\mathrm{SOS}}$ and $\sigma_h^2 = \frac{\sigma_n^2}{\sigma_s^2 \|\mathbf{h}\|^2}$. Thanks to the source power imbalance, now matrix $\mathbf{H}$ is identifiable from $\mathbf{C}_{\mathrm{SOS}}$, as $\mathbf{\Delta}_{\mathrm{SOS}}$ contains different eigenvalues.

Obviously, if the power of the two sources is unbalanced, the total channel capacity is lower than that of equally balanced sources. This is the price to be paid for making the SOS-based method applicable and taking advantage of its extremely low computational requirements. However, in Sections 4 and 5, we will show that the best choice is $\gamma^2 \approx 0.6$ and that in this case the total channel capacity is quite close to the balanced case.

3.2. HOS-based approaches

The orthogonal MIMO channel matrix $\mathbf{H}$ can also be estimated from the eigendecomposition of matrices made up of HOS of the received signals without the need of unbalancing the source powers. Indeed, for a (2×1) observation vector, $\mathbf{x}$, the fourth-order cumulant matrix $\mathbf{C}_{\mathrm{HOS}}(\mathbf{M})$ is a (2×2) matrix with components

$$[\mathbf{C}_{\mathrm{HOS}}(\mathbf{M})]_{ij} = \sum_{k,\ell=1}^{2} \mathrm{cum}(x_i, x_j^*, x_k, x_\ell^*) m_{lk} \tag{9}$$

where m_{lk} $k, l = 1, 2$, denote the entries of a (2×2) matrix $\mathbf{M}$ and the fourth-order cumulant is defined by

$$\begin{aligned} \mathrm{cum}(x_1, x_2, x_3, x_4) = {} & E[x_1 x_2 x_3 x_4] - E[x_1 x_2]E[x_3 x_4] \\ & - E[x_1 x_3]E[x_2 x_4] - E[x_1 x_4]E[x_2 x_3] \end{aligned} \tag{10}$$

It has been proved in Reference [11] that, for the particular case of zero-mean signals, the cumulant matrix admits the following decomposition

$$\mathbf{C}_{\mathrm{HOS}}(\mathbf{M}) = \mathbf{H}\mathbf{\Delta}_{\mathrm{HOS}}(\mathbf{M})\mathbf{H}^{\mathrm{H}} \tag{11}$$

where $\rho_{4i} = \mathrm{cum}(s_i, s_i^*, s_i, s_i^*)$ is the kurtosis of the ith source and $\mathbf{\Delta}(\mathbf{M})$ is a diagonal matrix given by

$$\mathbf{\Delta}_{\mathrm{HOS}}(\mathbf{M}) = \mathrm{diag}(\rho_{41}\mathbf{h}_1^{\mathrm{H}}\mathbf{M}\mathbf{h}_1, \rho_{42}\mathbf{h}_2^{\mathrm{H}}\mathbf{M}\mathbf{h}_2) \tag{12}$$

Here, $\mathbf{h}_i$ is the ith column of $\mathbf{H}$, that is $\mathbf{h}_1 = [h_1 \;\; h_2^*]^{\mathrm{T}}$ and $\mathbf{h}_2 = [h_2 \;\; -h_1^*]^{\mathrm{T}}$. Since for the Alamouti coded scheme the channel matrix is orthogonal, $\mathbf{H}^{\mathrm{H}}$ diagonalises $\mathbf{C}_{\mathrm{HOS}}(\mathbf{M})$ for any $\mathbf{M}$ provided that $\mathbf{\Delta}(\mathbf{M})$ contains different entries, that is

$$L = \left|\rho_{41}\mathbf{h}_1^{\mathrm{H}}\mathbf{M}\mathbf{h}_1 - \rho_{42}\mathbf{h}_2^{\mathrm{H}}\mathbf{M}\mathbf{h}_2\right| \neq 0 \tag{13}$$

In particular, the approach proposed by Beres and Adve in Reference [10] considers the cases $m_{11} = 1$, $m_{12} = m_{21} = m_{22} = 0$; and $m_{11} = m_{12} = m_{21} = 0$ and $m_{22} = 1$. Assuming that the transmitted signals have the same kurtosis, we obtain from Equation (13) that the channel matrix is identifiable as long as $|h_1|^2 \neq |h_2|^2$.

As an extension of this approach, we propose to identify $\mathbf{H}$ by computing the eigenvectors of a linear combination of fourth-order cross-cumulant matrices. This can be obtained by using a matrix $\mathbf{M}$ with entries $m_{11} = 1$, $m_{12} = m_{21} = 0$ and $m_{22} = \lambda$, being λ a real valued parameter. From Equation (13), we conclude that this method allows to estimate $\mathbf{H}$ as long as

$$L = (1-\lambda)(|h_1|^2 - |h_2|^2) \neq 0 \tag{14}$$

Thus, the channel is identifiable if $\lambda \neq 1$ and $|h_1|^2 \neq |h_2|^2$. In particular, we propose the utilisation of $\lambda = -1$ since this choice provides a significant performance improvement with respect to the Beres and Adve approach in Reference [10], as will be shown in the following sections.

Another way to estimate the mixing matrix consists in performing a simultaneous diagonalisation of several fourth-order cumulant matrices, as the JADE algorithm [11]. This algorithm provides an excellent performance but, unfortunately, its computational load is very high. In Sections 4 and 5, the JADE algorithm will be used only as a benchmark.

4. COMPUTER SIMULATIONS

This section presents the results of several computer simulations carried out to evaluate the performance of the estimation algorithms proposed in Section 3. The experiments have been carried out by simulating the transmission of QPSK signals in Rayleigh-distributed randomly generated flat fading channels affected by additive white Gaussian noise (AWGN). We assume block fading where the channel remains constant during the transmission of a block of K symbols. The statistics in Equations (4) and (9) have been calculated by sample averaging over each

DOI: 10.1002/ett

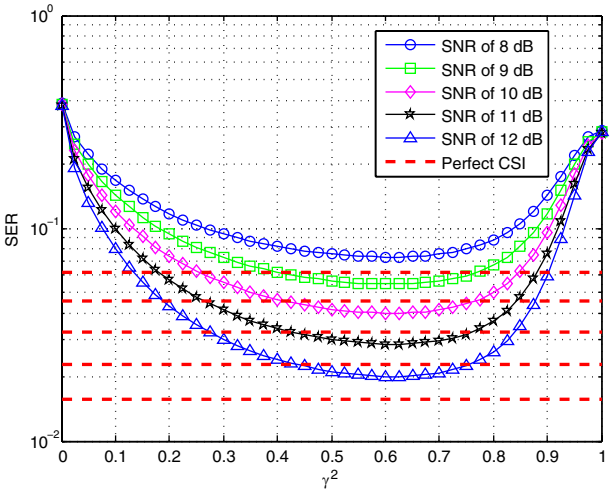

Figure 2. Computer simulations: SER *versus* γ^2 obtained with the SOS-based approach for QPSK signals and different values of SNR $= \sigma_s^2/N_0$. The horizontal dashed lines represent the SER obtained with perfect CSI.

block of symbols and the performance has been measured in terms of the symbol error rate (SER).

We have evaluated the performance of the SOS-based approach for several values of γ^2. Figure 2 shows the SER *versus* γ^2 for signal to noise ratio (SNR) values of 8, 9, 10, 11 and 12 dB. The autocorrelation matrix has been estimated with $K = 500$ symbols. This figure also plots the SER obtained with perfect CSI (horizontal dashed lines). It is apparent that the SOS-based channel estimation approach fails for $\gamma^2 = 1$ because this case corresponds to signals with the same power. The same occurs when $\gamma^2 = 0$ which corresponds to the limiting case where only s_1 is transmitted. Note also that the best performance is obtained with $\gamma^2 \approx 0.6$.

Figure 3 shows the SER *versus* SNR curves of a (2×1) Alamouti coded QPSK system using different methods for the channel estimation: Beres *et al.*, JADE, the novel SOS approach with $\gamma^2 = 0.6$ and the novel HOS approach with $\lambda = -1$. The system performance with perfect CSI is also plotted as a benchmark. The SER curves were obtained by simulating data blocks of $K = 500$ symbols and by averaging the results for 10 000 different realisations. Note that the method proposed by Beres *et al.* is outperformed by the novel HOS approach. However, notice the poor performance of HOS-based methods in the high SNR regime when compared with the novel SOS approach. It is apparent from Figure 3 the superior performance of the SOS approach since it only incurs in a 0.5 dB penalty with respect to the perfect CSI case.

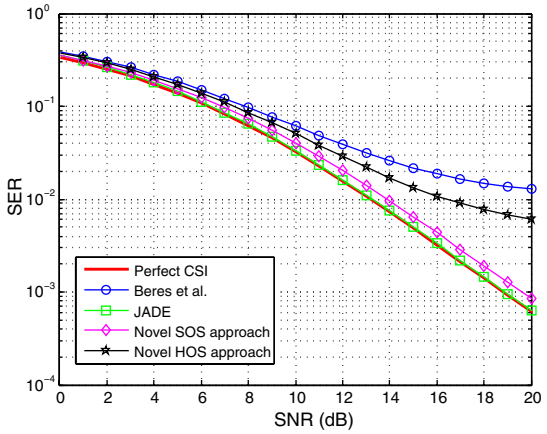

Figure 3. Computer simulations: SER *versus* SNR obtained with the different channel estimation methods.

It is still possible to obtain an even better performance, almost reaching the optimum curve, by using the JADE algorithm (see Figure 3). However, notice the high complexity of the JADE algorithm illustrated in Figure 4 that shows the execution time required to compute 10^4 channel estimates, as a function of the block size. On the other hand, the SOS method exhibits the lowest complexity, which remains almost constant with the block size. Figure 4 also shows the higher complexity of the proposed HOS method with respect to that of Beres *et al.* Thus, we can conclude that the SOS approach exhibits an excellent trade-off between performance and complexity.

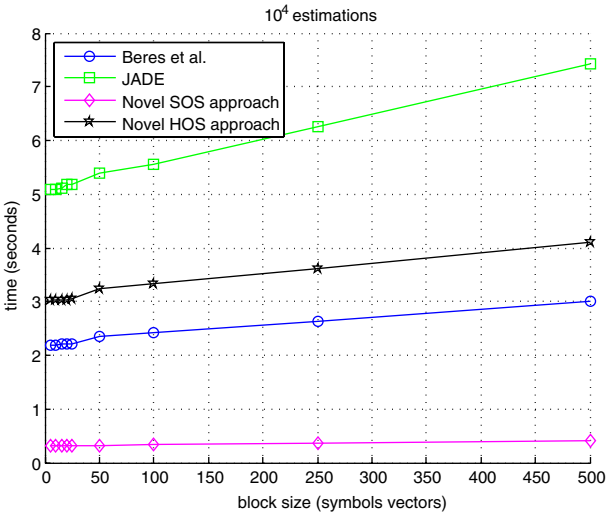

Figure 4. Time required to process 10^4 blocks.

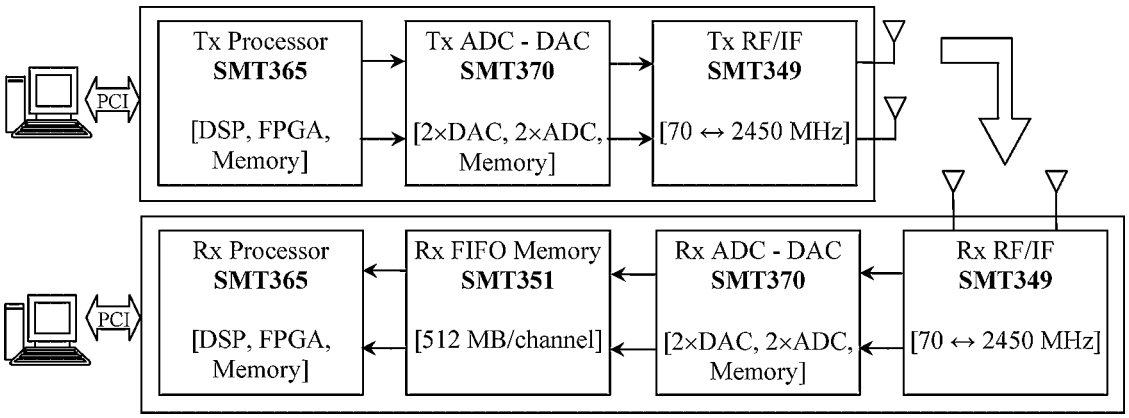

Figure 5. Schematic diagram of the MIMO testbed employed in the experiments.

5. TESTBED RESULTS

5.1. Description of the (2 × 2) *MIMO testbed*

Figure 5 shows a diagram of the Testbed PCs. The hardware testbed is based on a PCI carrier board SMT310Q and a basic processing module: the SMT365 equipped with a Xilinx Virtex-II FPGA and a Texas Instruments C6416 DSP at 600 MHz. The processing module has two buses that can transfer 32-bit words up to 400 MB/s, allowing the connection with the SMT370 module, that contains a dual AD9777 D/A converter and two AD6645 A/D converters. The SMT370 module also has a 2 MB per-channel memory that is used to load the frames to be transmitted. At the receiver side, the data acquired by the A/D converters is stored in real time in a 1 GB FIFO memory SMT351 module and, in an off-line task, passed to the middleware through the PCI bus. Finally, the testbed contains two SMT349 RF front-end modules. They perform the up and down conversion operations from an 70 MHz Intermediate Frequency (IF) to a 2.45 GHz carrier RF, with 16 MHz of maximum bandwith. In order to synchronise both the transmitter and the receiver, a simple synchronisation protocol is implemented over a common Ethernet connection. When the transmitter sends data over the channel, it also sends a control signal to the receiver in order to start the signal acquisition process.

5.2. Experiments setup

The MIMO testbed described before has been used to test the estimation methods described in Section 3. Figure 6 shows the block diagram of the (2 × 1) Alamouti coded system with QPSK modulation implemented on the testbed. During the experiments, we generated 1000 QPSK symbols of each source (s_1 and s_2). The first subframe of (2 × 500) symbols is used to test the HOS-based methods. The second subframe, also composed by (2 × 500) symbols, is employed to test the SOS-based method. The power of the second subframe is unbalanced before the Alamouti encoder according to Equation (6).

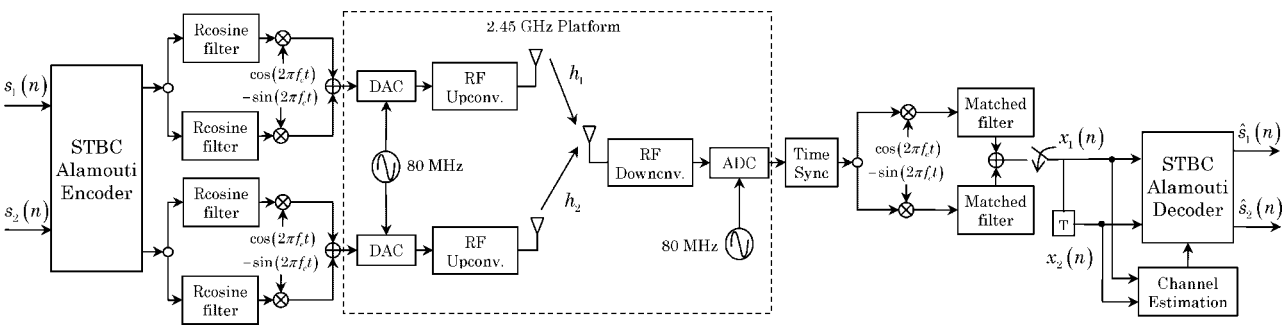

Figure 6. Block diagram of the implemented 2 × 1 Alamouti coded QPSK system.

DOI: 10.1002/ett

As a performance bound, we have also evaluated the system performance when using LS channel estimation [15] considering that all symbols of the first subframe are used for training. Subsequently, LS estimation has been used to decode only this subframe. Therefore, its performance is very close to the case where perfect CSI is available at reception.

After the Alamouti encoder, symbols were IQ modulated using 16 samples per symbol, a square root raised cosine pulse shaping with a roll-off factor of 40 per cent and a discrete-time IF of 0.125. Passing this signal through a D/A converter configured with a clock frequency of 80 MHz yields to a QPSK analogue signal of 5 MBauds symbol rate, 7 MHz bandwidth and 10 MHz carrier frequency. Finally, the replica at 70 MHz is filtered out and up converted to a carrier RF frequency of 2.45 GHz.

With the aim of achieving a correct time synchronisation, a 50 pseudo-random symbol sequence is added at the beginning of the frame obtained after the Alamouti encoder. The preamble sequence is only transmitted by one of the two antennas while the other is idle. The resulting frame is thus composed of a 50 symbol preamble 4000 data symbols (2000 information symbols). Since we are using 16 samples per symbol, the frame contains 65 600 16-bit signal samples which results in a frame size equal to 128 125 Kbytes. At the receiver, the known preamble is correlated with the acquired signal to determine the first frame sample. Also a carrier recovery step must be incorporated after the time synchronisation to correct signal frequency impairments due to reference oscillator misadjustments. After IQ demodulation, a root raised cosine-matched filter is used in each demodulator branch followed by a down sampler to produce the I and the Q components of the baseband signal.

In order to experimentally obtain SER *versus* SNR curves for each estimation method, every frame is sent several times with different transmitting power. Different channel realisations and distinct signal strength values are obtained in this manner. In a later step, the SNR is estimated for each received frame jointly with the SER obtained by the estimation method. Finally, the pairs formed by the SNR with its corresponding SER are sorted by SNR value and plotted to obtain a performance curve.

5.3. *Scenario 1: line of sight (LOS)*

Figure 7 shows a schematic diagram of the room layout and the antenna locations where we carried out the experiments. The transmitter and the receiver were approximately 5 m away from each other with a clear LOS between them.

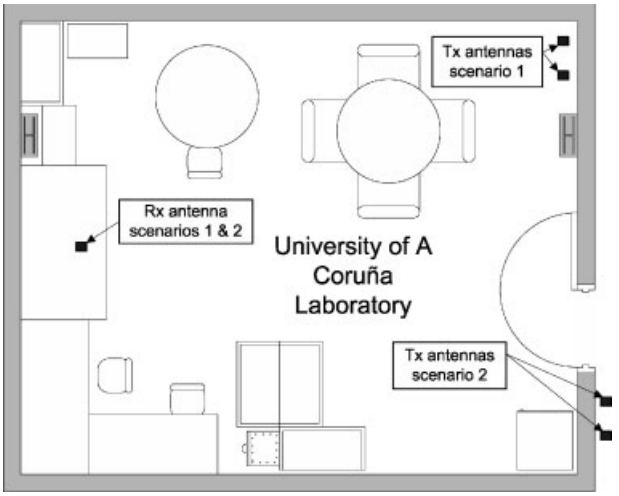

Figure 7. Experimental setup, showing the room layout and the antenna locations.

The transmitting antennas were separated about 30 cm from each other, in order to provide a good spatial diversity.

In order to apply the SOS-based approach proposed in Subsection 3.1, the optimum value of the source power unbalance parameter γ^2 must be found. To this end, the SER was evaluated for different values of γ^2. The results are plotted in Figure 8 for the LOS scenario and show that the optimal value is around $\gamma^2 = 0.64$. This value is in accordance with that obtained by simulations over an uncorrelated Rayleigh channel. In the experiments that follow, we set $\gamma^2_{\text{opt}} = 0.64$.

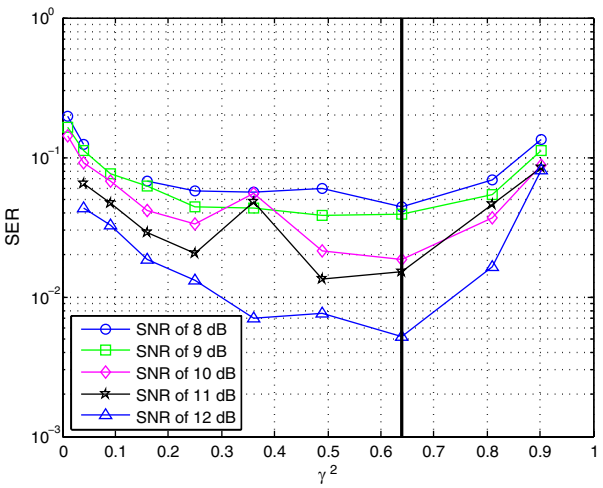

Figure 8. LOS scenario: performance of the SOS-based method as a function of parameter γ^2.

DOI: 10.1002/ett

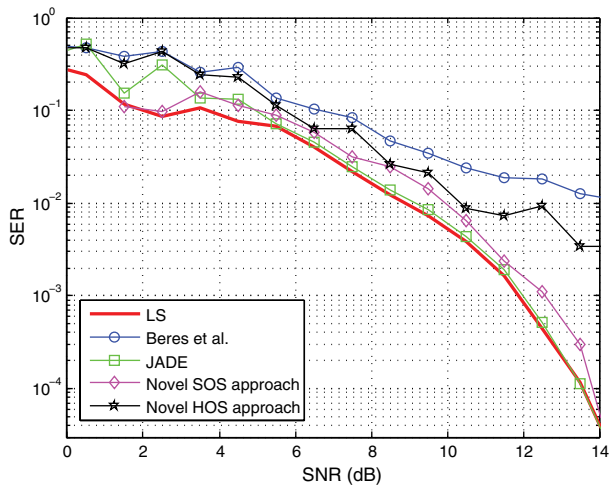

Figure 9. LOS scenario: SER performance *versus* SNR.

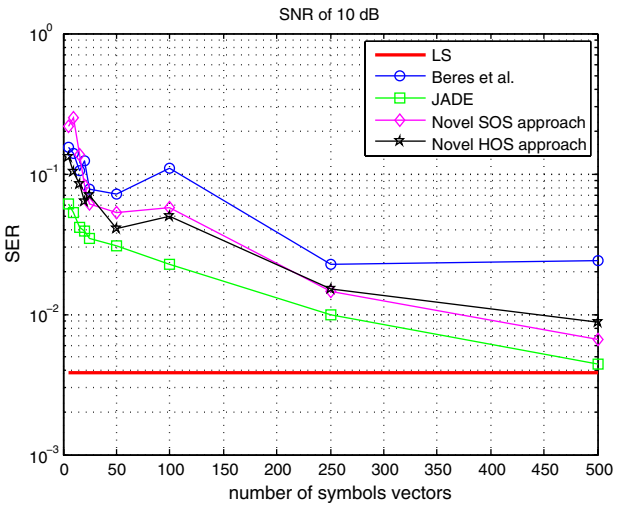

Figure 10. LOS scenario: computational efficiency of the channel estimation methods in terms of SER as a function of the number of used symbols.

Figure 9 shows the obtained SER *versus* SNR curves for a block size $K = 500$ and different methods for channel estimation: JADE, Beres *et al.*, the novel SOS approach with $\gamma^2 = 0.64$ and the novel HOS approach with $\lambda = -1$. Notice that, similarly to the results obtained with computer simulations, the JADE algorithm achieves the same performance as with LS estimation while the SOS-based approach differs in just about 0.5 dB. Figure 9 also shows the poorer performance of HOS methods since they present a flooring effect for SNR values greater than 10 dB. Nevertheless, the performance of the HOS-based method proposed by the authors is better than that of the one proposed by Beres and Adve [10].

In order to evaluate the convergence speed of the channel estimation methods, we calculated the SER for different number of symbols employed to estimate the statistics in Equations (4) and (9), at an SNR of 10 dB. The results are plotted in Figure 10. Notice, again, the superior performance of the SOS-based approach with respect to those based on HOS and its proximity to JADE.

5.4. Scenario 2: non-line of sight

We implemented a second scenario without LOS, where the transmitter was placed about 9 m away from the receiver (see Figure 7). The transmitting antennas were still separated about 30 cm from each other.

Figure 11 illustrates the SER in the non-LOS (NLOS) scenario as a function of the received SNR for a block size $K = 500$ and the different channel estimation methods. Contrarily to the LOS scenario, both the novel SOS and HOS methods perform adequately showing a penalty with respect to the LS case lower than 1 dB. Again, JADE is the method that exhibits better performance whereas the HOS-method proposed by Beres and Adve [10] shows the worst.

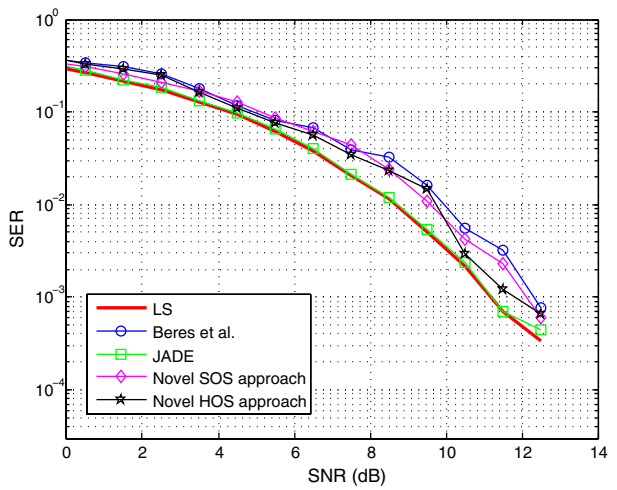

Figure 11. NLOS scenario: SER performance *versus* SNR.

6. CONCLUSIONS

The experimental performance of several blind channel estimation techniques for Alamouti coded systems with one receiving antenna has been evaluated in this paper. The considered techniques exploit the orthogonality property

DOI: 10.1002/ett

of the effective MIMO channel matrix through the eigendecomposition of matrices made up of SOS or HOS of the received signals. The algorithms were tested *via* computer simulations and on real data obtained from indoor scenarios using a MIMO hardware platform working at 2.4 GHz. Both simulations and realistic experiments in LOS and NLOS scenarios show that the proposed SOS-based method exhibit a performance penalty of less than 1 dB when compared with the case of perfect CSI. Thus, we can conclude that the SOS approach exhibits an excellent compromise quality between channel estimation and computational complexity.

ACKNOWLEDGEMENTS

This work has been partially supported by Xunta de Galicia, Ministerio de Educación y Ciencia of Spain and FEDER funds of the European Union under grants number PGIDT06TIC10501PR and TEC2007-68020-C04-01.

REFERENCES

1. Gesbert D, Shafi M, Shan-Shiu D, Smith PJ, Naguib A. From theory to practice: an overview of MIMO space-time coded wireless systems. *IEEE Journal on Selected Areas in Communications* 2003; **21**:281–302.
2. Jafarkhani H. *Space Time Coding*. Cambridge University Press: Cambridge, UK, 2005.
3. Alamouti SM. A simple transmit diversity technique for wireless communications. *IEEE Journal on Selected Areas in Communications* 1998; **16**:1451–1458.
4. Tarokh V, Jafarkhani H, Calderbank AR. Space-time block codes from orthogonal designs. *IEEE Transactions on Information Theory* 1999; **45**(5):1456–1467.
5. Larsson EG, Stoica P. *Space-Time Block Coding for Wireless Communications*. Cambridge University Press: Cambridge, UK, 2003.
6. Sandhu S, Paulraj A. Space-time block codes: a capacity perspective. *IEEE Communications Letter* 2000; **4**(12):384–386.
7. Andrews JG, Ghosh A, Muhamed R. *Fundamentals of WiMAX: Understanding Broadband Wireless Networking*. Prentice Hall Communications Engineering and Emerging Technologies Series, 2007.
8. Hughes BL. Differential space-time modulation. *IEEE Transactions on Information Theory* 2000; **46**(7):2567–2578.
9. Pérez-Iglesias HJ, Dapena A, Castedo L, Zarzoso V. Blind channel identification for Alamouti's coding systems based on eigenvector decomposition. In *Proceedings of 13th European Wireless Conference*, Paris, France. April 2007.
10. Beres E, Adve R. Blind channel estimation for orthogonal STBC in MISO systems. In *Proceedings of Global Telecommunications Conference, 2004*, Vol. 4, November 2004; pp. 2323–2328.
11. Cardoso J-F, Souloumiac A. Blind beamforming for non-Gaussian signals. In *IEE Proceedings-F*, Vol. 140, no. 6, December 1993; pp. 362–370.
12. Shahbazpanah S, Gershman AB, Manton J. Closed-form blind MIMO channel estimation for orthogonal space-time block codes. *IEEE Transactions on Signal Processing* 2005; **53**(12): 4506–4516.
13. Vía J, Santamaría I, Pérez J, Ramírez D. Blind decoding of MISO-OSTBC systems based on principal component analysis. In *Proceedings of International Conference on Acoustic, Speech and Signal Processing*, Vol. IV, 2006; pp. 545–549.
14. García-Naya JA, Fernández-Caramés T, Pérez-Iglesias H, *et al*. Performance of STBC transmissions with real data. In *Proceedings of 16th IST Mobile and Wireless Communications Summit*, Budapest, Hungary, July 2007.
15. Naguib AF, Tarokh V, Seshadri N, Calderbank AR. A space-time coding modem for high-data-rate wireless communications. *IEEE Journal on Selected Areas in Communications* 1998; **16**(8):1459–1478.

DOI: 10.1002/ett